

## Oxidation Reactions

# *tert*-Butyl as a Functional Group: Non-Directed Catalytic Hydroxylation of Sterically Congested Primary C–H Bonds

Siu-Chung Chan, Andrea Palone, Massimo Bietti,\* and Miquel Costas\*

**Abstract:** The *tert*-butyl group is a common aliphatic motif extensively employed to implement steric congestion and conformational rigidity in organic and organometallic molecules. Because of the combination of a high bond dissociation energy (~100 kcal mol<sup>-1</sup>) and limited accessibility, in the absence of directing groups, neither radical nor organometallic approaches are effective for the chemical modification of *tert*-butyl C–H bonds. Herein we overcome these limits by employing a highly electrophilic manganese catalyst, [Mn(CF<sub>3</sub>bpeb)(OTf)<sub>2</sub>], that operates in the strong hydrogen bond donor solvent nonafluoro-*tert*-butyl alcohol (NFTBA) and catalytically activates hydrogen peroxide to generate a powerful manganese-oxo species that effectively oxidizes *tert*-butyl C–H bonds. Leveraging on the interplay of steric, electronic, medium and torsional effects, site-selective and product chemoselective hydroxylation of the *tert*-butyl group is accomplished with broad reaction scope, delivering primary alcohols as largely dominant products in preparative yields. Late-stage hydroxylation at *tert*-butyl sites is demonstrated on 6 densely functionalized molecules of pharmaceutical interest. This work uncovers a novel disconnection approach, harnessing *tert*-butyl as a potential functional group in strategic synthetic planning for complex molecular architectures.

## Introduction

Because of the biological and pharmaceutical significance of oxygenated hydrocarbon frames and of the opportunities offered by C(sp<sup>3</sup>)–O bonds for follow-up chemical elabo-

ration, C(sp<sup>3</sup>)–H bond oxygenation is an extensively investigated transformation.<sup>[1–6]</sup> Selecting among multiple non-equivalent C–H bonds in organic molecules, and in particular targeting stronger bonds over weaker and intrinsically more activated ones, stand as some of the main challenges associated to the development of C–H functionalization methods.<sup>[7–13]</sup> Such transformations would make accessible so far unconsidered paths allowing the streamlined synthetic elaboration of organic molecules.

From a thermodynamic perspective, the reactivity trend operating in hydrogen atom transfer (HAT) reactions mediated by radical and radical-like reagents such as metal-oxo species is greatly influenced by the C–H bond dissociation energies (BDEs) that typically follow the order: tertiary > secondary > primary (Scheme 1A).<sup>[14]</sup> In contrast, in precious metals mediated C(sp<sup>3</sup>)–H bond functionalization proceeding through the formation of an organometallic intermediate, an opposite reactivity trend is observed, dictated by the strength of the resultant M–C bond (Scheme 1B).<sup>[15–18]</sup>

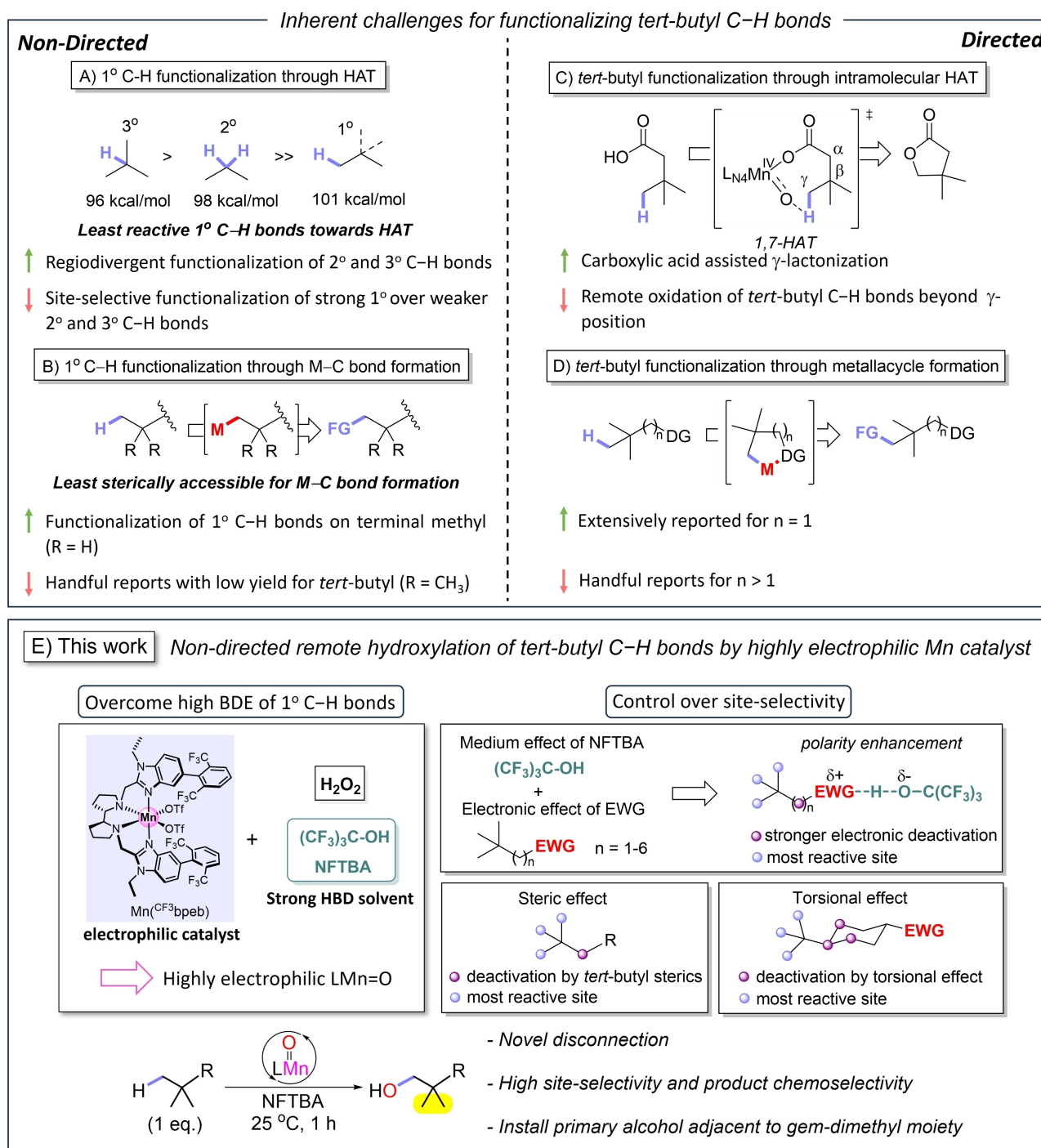
The *tert*-butyl group is a common molecular motif used to implement steric hindrance and structural rigidity in organic and organometallic molecules.<sup>[19]</sup> However, in terms of reactivity, the *tert*-butyl C–H bonds represent a special case. The singular combination of high BDE and steric encumbrance make *tert*-butyl C–H bonds generally unreactive against both HAT and organometallic operating reagents.<sup>[13,20–21]</sup> In addition, in the presence of these structural units, ‘chain walking’ reactions cannot be employed due to the impossibility of M–H migration through the *tert*-butyl quaternary carbon.<sup>[22–24]</sup> As a result, there is a lack of synthetic methodology for the non-directed selective functionalization of *tert*-butyl C–H bonds, and the synthetic potential of this transformation has been so far overlooked.

Interestingly, the oxidation of *tert*-butyl C–H bonds of bioactive molecules has been reported in enzymatic reactions involving iron oxygenases that operate via hypervalent iron-oxo species,<sup>[25–27]</sup> suggesting that these species may be suitable oxidants to address this challenging problem. Manganese complexes bearing aminopyridine ligands are powerful catalysts that, in the presence of hydrogen peroxide, oxidize C(sp<sup>3</sup>)–H bonds via reaction mechanisms that resemble oxygenases and entail HAT executed by high valent manganese-oxo species.<sup>[28–31]</sup> Structural and electronic tuning of these catalysts, combined with medium effects<sup>[32–35]</sup> can be employed to manipulate the chemoselectivity of the reaction, offering a powerful tool for selective functionalization. We have recently described that these complexes effectively catalyze the intramolecular  $\gamma$ -lactonization of

[\*] S.-C. Chan, A. Palone, M. Costas  
Institut de Química Computacional i Catàlisi (IQCC) and Departament de Química, Universitat de Girona,  
Campus Montilivi, Girona E-17071, Catalonia, Spain  
E-mail: miquel.costas@udg.edu

M. Bietti  
Dipartimento di Scienze e Tecnologie Chimiche, Università “Tor Vergata”, Via della Ricerca Scientifica, 1 I-00133 Rome, Italy  
E-mail: bietti@uniroma2.it

© 2024 The Authors. Angewandte Chemie International Edition published by Wiley-VCH GmbH. This is an open access article under the terms of the Creative Commons Attribution License, which permits use, distribution and reproduction in any medium, provided the original work is properly cited.



different factors operating in the HAT step may be used to achieve high levels of selectivity in the hydroxylation of *tert*-butyl C–H bonds in substrates containing multiple functionalities. Understanding of these factors and their rational application provides valuable guidelines for expanding the scope of non-directed C(sp<sup>3</sup>)–H oxidation reactions. The reaction installs a primary alcohol adjacent to a *gem*-dimethyl motif and serves as an orthogonal approach for functionalization of the *tert*-butyl group for further synthetic elaboration.

## Results and Discussion

### Reaction Development on 2,2,3,3-Tetramethylbutane (1)

2,2,3,3-Tetramethylbutane, **1** was chosen for reaction development. The oxidation of **1** (0.1 M) was initially conducted using 1 eq. of H<sub>2</sub>O<sub>2</sub> (0.35 M in NFTBA) delivered over 30 min by syringe pump to an open-to-air vial containing 17.5 eq. of AcOH and 1 mol% of the Mn catalyst in a NFTBA stirred solution at 25 °C for a total reaction time of 1 hour. A series of manganese catalysts bearing tetraazadentate ligands, containing pyridine or benzimidazole donors, were employed (Figure 1A). In all cases, the reaction delivered 2,2,3,3-tetramethylbutanol (**P1\_1°-OH**) as the major product accompanied by minor amounts of 2,2,3,3-tetramethylbutanal (**P1\_CHO**) and 2,2,3,3-tetramethylbutanoic acid (**P1\_COOH**). In general, improved yields were obtained when employing sterically encumbered catalysts (compare entry 1 with entries 3 and 4, and entry 5 with entries 6 and 7). Notably, the catalyst bearing the ligand anchored with electron-withdrawing substituents, Mn(CF<sub>3</sub>bpeb) gave the best performance delivering **P1\_1°-OH** in 51 % yield accompanied by a trace amount (2 %) of **P1\_CHO** as overoxidation product, achieving 96 % product selectivity (entry 7; throughout this work, product selectivity is defined as yield of specific product/total product yield). In sharp contrast, when the iron catalyst analogue Fe(CF<sub>3</sub>bpeb) was employed, <1 % of oxidation products were observed (see SI, Table S1). A progressive decrease in both product selectivity and mass balance were observed with decreasing solvent HBD ability, i.e. going from NFTBA to 1,1,1,3,3,3-hexafluoro-2-propanol (HFIP), 2,2,2-trifluoroethanol (TFE) and CH<sub>3</sub>CN (Figure 1B). Accordingly, the relative amount of the overoxidized carboxylic acid (**P1\_COOH**) and  $\gamma$ -lactone (**P1\_Lac**) products, that were not observed in NFTBA, are detected in trace amounts (<2 %) in HFIP, and become the exclusive products observed, albeit in low overall yield, in CH<sub>3</sub>CN. These observations highlight the synergistic contribution of the electrophilic Mn(II) catalyst and solvent HBD ability in achieving the hydroxylation product **P1\_1°-OH** in high yield and product selectivity. Presumably, the very strong HBD character of NFTBA plays a dual function: 1) it enhances the electrophilicity of the Mn-oxo catalyst through interaction with the ligand set;<sup>[43]</sup> and 2) induces a polarity reversal effect in the first formed alcohol product, that prevents overoxidation.<sup>[32,34]</sup>

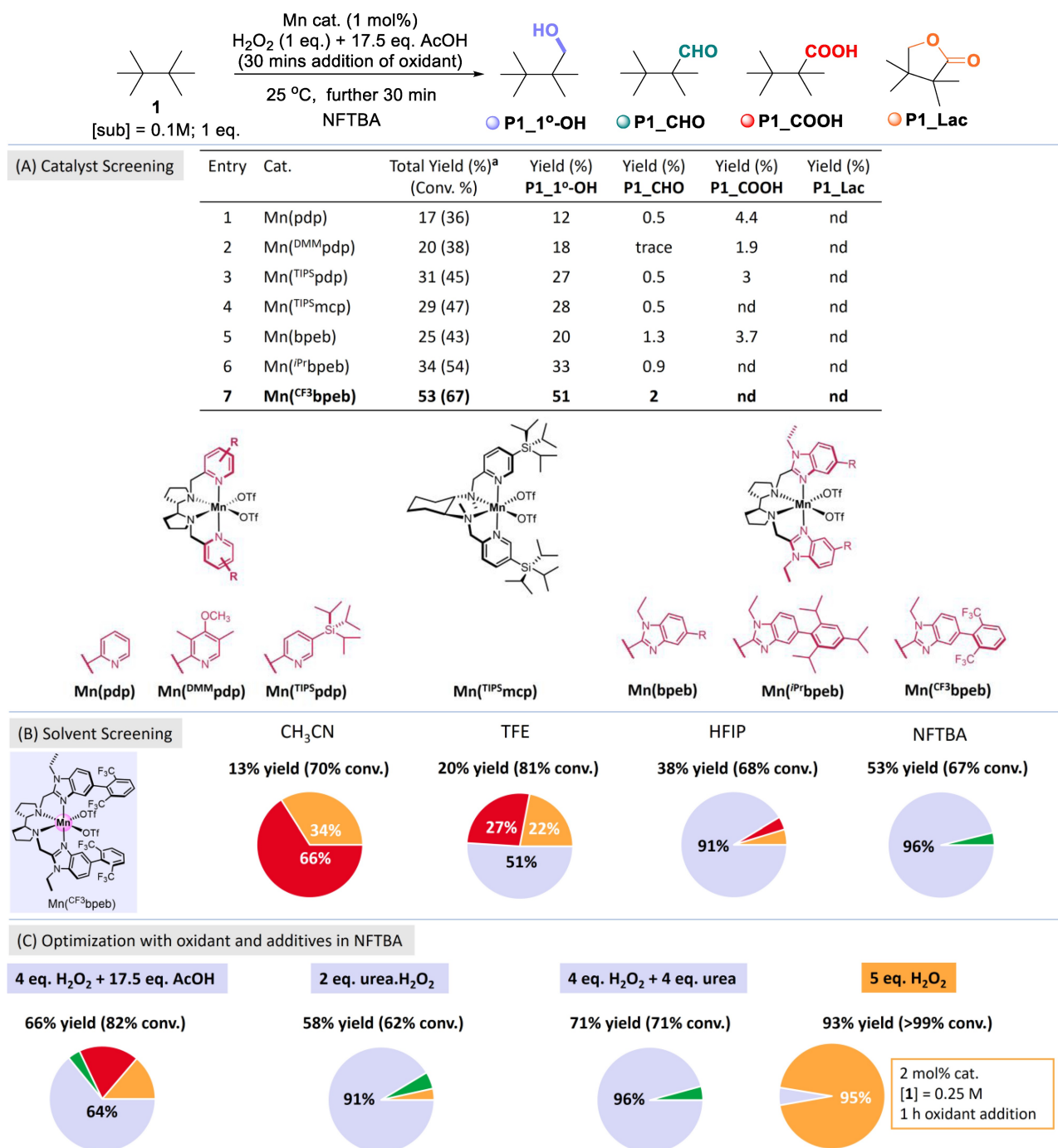
Further optimization targeting the amount of oxidant, catalyst and carboxylic acid loading and substrate concentration did not improve the reaction outcome. (Table S3). However, overall yield, product selectivity and mass balance could be improved to 71 %, 96 % and >99 %, respectively when replacing acetic acid by urea (4 eq.) (Figure 1C). These results point toward an important role played by urea HBD ability in preventing overoxidation of **P1\_1°-OH**.<sup>[44]</sup> In contrast, lactone **P1\_Lac**, deriving from intramolecular lactonization in the overoxidized product **P1\_COOH** was obtained in excellent yield (88 %) and outstanding selectivity over **P1\_1°-OH** (95 %) in the absence of AcOH, employing higher H<sub>2</sub>O<sub>2</sub> (5 eq.) and catalyst loadings (2 mol %), 0.25 M substrate concentration and a longer oxidant addition time (1 h). The reaction is particularly notable because it entails the one-pot consecutive and highly selective oxidation of two primary C–H bonds.

### Effect of *tert*-Butyl Sterics on Site-Selectivity

We then explored the effect of *tert*-butyl sterics on the competition between primary and secondary C–H bond oxidation.<sup>[4,7,45–47]</sup> For this purpose, 2,2,4,4-tetramethylpentane (**2**) and 2,2,5,5-tetramethylhexane (**3**) were selected as substrates. Oxidation of both **2** and **3** exclusively delivered products deriving from primary C–H bond oxidation despite the presence of weaker and intrinsically more activated secondary C–H bonds (Figure 2a). Reactions proceeded with very good mass balance, delivering the primary alcohols deriving from *tert*-butyl C–H bond hydroxylation (**P2\_1°-OH** and **P3\_1°-OH**) in 60 % and 53 % yield, respectively, and  $\geq$ 91 % product selectivity over overoxidized aldehyde and diol products. These observations clearly indicate that methylenic units adjacent to *tert*-butyl groups are effectively shielded by steric congestion that prevents their functionalization. The significance of the yields and product selectivities obtained in these reactions are best appreciated when compared with state-of-the-art literature (Figure 2b). For instance, with **2** both copper-mediated and metal-free C–H bond borylation has been reported using a 5 eq. substrate excess, yielding 84 and 40 % of the primary borylated product, respectively, with 97 % selectivity over the secondary ones.<sup>[48–49]</sup> Moreover, Hartwig and co-workers have recently shown that oxidation of **2** with 2,6-dichloropyridine *N*-oxide catalysed by a ruthenium porphyrin, proceeds selectively at the methylenic site, further supporting the unique selectivity for the *tert*-butyl site attained by our catalytic system.<sup>[50]</sup>

### Remote Selectivity Induced by Electronic Effects of Functional Groups

Due to the electrophilic nature of metal-oxo species, it is well established that electron-withdrawing groups (EWGs) in the substrate can deactivate proximal C–H bonds toward HAT to these reagents by a polarity mismatching effect.<sup>[12,51]</sup> To systematically evaluate the impact of these groups on the

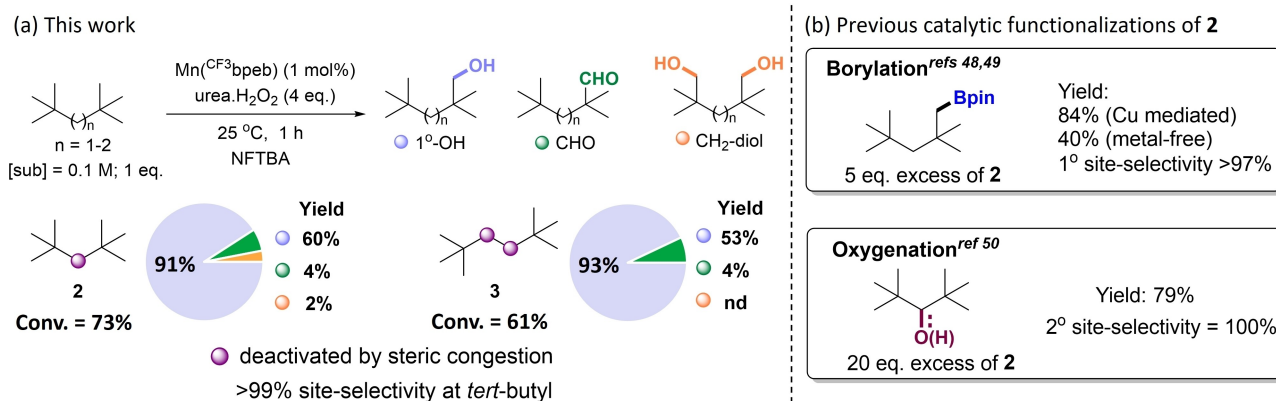


**Figure 1.** Reaction development on **1**: (A) Catalyst screening. (B) Solvent screening. (C) Optimization with oxidant and additives. <sup>a</sup>Initial conditions: 1 eq. of substrate (0.1 M), Mn catalyst (1 mol%) and AcOH were dissolved in NFTBA; 1 eq. of H<sub>2</sub>O<sub>2</sub> (0.35 M in NFTBA) was delivered over 30 min with a syringe pump followed by additional 30 min reaction time at 25 °C, unless otherwise indicated. Catalysts enantiomers were used interchangeably. Substrate conversion and product yields were determined by GC-FID with biphenyl as internal standard. The yields presented in (B) and (C) correspond to the sum of all oxidation products obtained by using Mn(CF<sub>3</sub>bpeb) as catalyst. The pie charts indicate product selectivity. Full reaction details are available in the SI, Tables S1–S6.

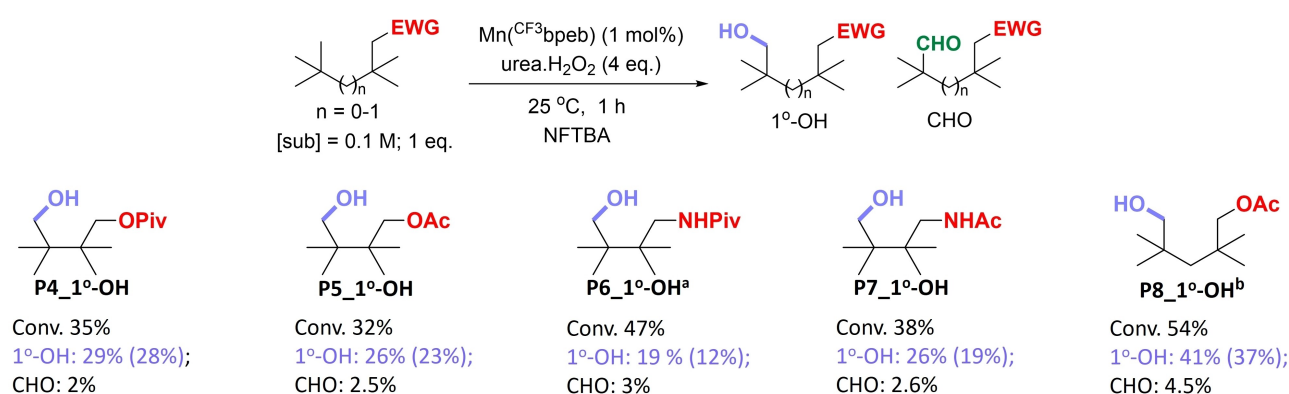
oxidation of *tert*-butyl C–H bonds, 1-(2,2,3,3-tetramethyl)-butylpivalate, acetate, pivalamide and acetamide (**4–7**, respectively) and 1-(2,2,4,4-tetramethyl)pentylacetate (**8**) were used to examine the oxidation site-selectivity, and results compared with those obtained for **1** and **2**, respectively. Reactions were performed using 4 eq. of urea.H<sub>2</sub>O<sub>2</sub> as

oxidant (Figure 3). In all cases, predominant formation of the alcohol product deriving from hydroxylation at a remote primary C–H bond was observed in modest yield (19–29 %) and very good product selectivity (86–91 %), while products resulting from oxidation at the methylenic site adjacent to the functional group were detected in only trace amounts





**Figure 2.** (a) Effect of *tert*-butyl sterics on the oxidation of **2** and **3** in this work. The pie charts indicate product selectivity while individual product yields are indicated by the small circles. Substrate conversion and product yields were determined by GC-FID with biphenyl as internal standard. Full reaction details are available in the SI, Table S7 and S8. (b) Previous work describing catalytic C–H bond functionalization of **2**.



**Figure 3.** Effect of EWGs on the oxidation of **4–8**. Substrate conversion and product yields were determined by GC-FID with biphenyl as internal standard. Isolated yields are indicated in parentheses. [a] 2 mol % cat. [b] 99% site-selectivity at *tert*-butyl C–H bonds. Full details on the reactions and associated product distributions are available in the SI, Tables S9–S18.

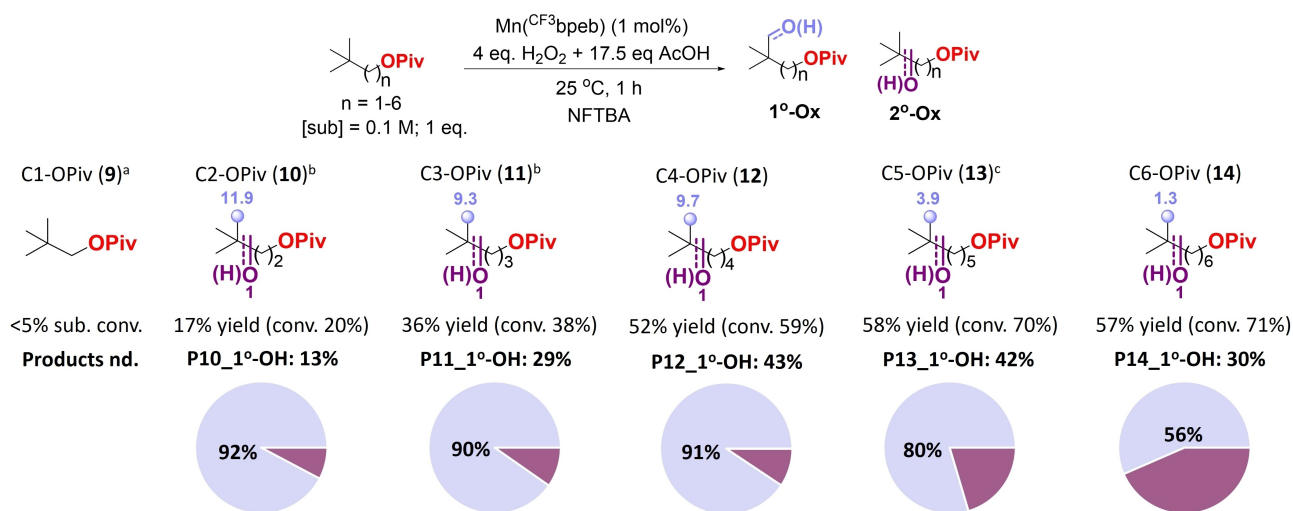
(<1%). Of notice, product yields are greatly decreased when compared to the corresponding oxidations of **1** and **2**, reflecting electronic deactivation of the primary C–H bonds.

Along this line, a significant increase in yield was observed going from **5** to **8**, where OAc is moved one carbon away from the *tert*-butyl group, a behaviour that can be accounted for on the basis of a reduced electronic deactivation determined by the remote EWG. Notably, **P8\_1°-OH** could be obtained in 41% yield along with 4.5% of the corresponding formyl derivative, showing that oxidation occurs with exquisite site-selectivity and compares positively with the 26% yield of **P5\_1°-OH** obtained in the oxidation of **5**. However, the lower steric demand associated with a larger rotational freedom in **8** may also account for this improvement.<sup>[52]</sup>

Solvent induced polarity enhancement has been recently described as an effective strategy to enhance selectivity for oxidation at the most remote methylenic site of linear alkyl chains bearing terminal EWGs.<sup>[53–55]</sup> For instance, oxidation of 1-heptyl derivatives by Mn(<sup>TIPS</sup>mcp) in NFTBA led to predominant functionalization (up to 88% site-selectivity) at the most remote (C6) methylenic site.<sup>[55]</sup> However, with 1-

pentyl, 1-hexyl and 1-heptyl derivatives, the primary C–H bonds at the terminal methyl group were never oxidized. Replacing the terminal ethyl by a *tert*-butyl is envisaged as a strategy to invert the selectivity between primary and secondary C–H bonds because of the specific structural characteristics of the latter group. In first place, the steric hindrance exerted by the *tert*-butyl group prevents oxidation at the adjacent and most remote methylenic site, as seen in the oxidations of **2**, **3** and **8**. As a result of the presence of a quaternary carbon, compared to the linear derivative, the first accessible methylenic site is now moved two positions closer to the deactivating EWG, further magnifying electronic differences between competing primary and secondary sites. Finally, a statistic factor plays moreover in favour of primary C–H bond oxidation because of the 9 equivalent *tert*-butyl C–H bonds.

To explore the limits of the selectivity toward primary sites determined by polarity enhancement, the substrate scope was expanded to a series of alkyl pivalates bearing a terminal *tert*-butyl group (substrates **Cn**-OPiv, **9–14** in Figure 4; *n* = number of methylene spacers between *tert*-butyl and OPiv functionality), where competition for oxidation at



**Figure 4.** *C<sub>n</sub>*-OPiv substrates from C1 to C6 were selected to investigate the distal electronic effect on oxidation of *tert*-butyl C–H bonds. Substrate conversion and product distribution were determined by GC-FID with biphenyl as internal standard. [a] 5 mol % of catalyst. [b] 2 mol % of catalyst. [c] 1,3,5-trimethoxybenzene was used as internal standard for GC-FID. The pie charts indicate site-selectivity. Full reaction details are available in the SI, Tables S19–S30.

remote methylenic sites is anticipated to increase with increasing distance between the *tert*-butyl and OPiv groups. When C1-OPiv (**9**) was oxidized, >95 % substrate was recovered without detection of oxidation products, in line with the strong electronic deactivation of all primary and secondary C–H bonds. A progressive increase in substrate conversion and oxidation yield was observed with increasing the number of methylene spacers from C2 to C6, accompanied however by a decrease in the primary site-selectivity ratio (1° *sr*; relative ratio of oxidation products derived from *tert*-butyl C–H over other C–H bonds). A >9 1° *sr* is maintained for C2-OPiv (**10**), C3-OPiv (**11**) and C4-OPiv (**12**). A progressive decrease in 1° *sr* was observed with increasing number of methylenic spacers, 1° *sr*=3.9 and 1.3, respectively for C5-OPiv (**13**) and C6-OPiv (**14**), reflecting the increased competition for oxidation at secondary C–H bonds. Notably, 1°-OH remain the predominant products from C2-OPiv to C6-OPiv and in all cases the corresponding overoxidation products account for <4 %. Product yields also consistently respond to the proximity of the reactive site to the EWG. A progressive increase in yield of the 1°-OH product from C2-OPiv (13 %) to C4-OPiv (43 %) was observed, which represents the highest 1°-OH yield within the *C<sub>n</sub>*-OPiv series (see SI, Table S28 for details about the oxidation C3-OPiv to C5-OPiv in different solvent media).

Building on these results, the substrate scope was further expanded to other EWGs as hydrogen bond acceptors (HBA). The catalytic oxidation of substrates *C<sub>n</sub>*-EWG in NFTBA are presented in Table 1. The data shows that the 1° *sr* is influenced by the nature of the EWG. Replacing OPiv by more electron withdrawing 4-nitrobenzoate (4-NBz), 3,5-dinitrobenzoate (3,5-DNBz) or CN, the 1° *sr* increases substantially. For instance, the oxidation of C4-3,5-DNBz (**15**) and C4-CN (**21**) proceeded with two of the highest 1° *sr* (14.8 and 13.8 respectively) among the *C<sub>n</sub>*-EWG substrates. This improvement is even more significant

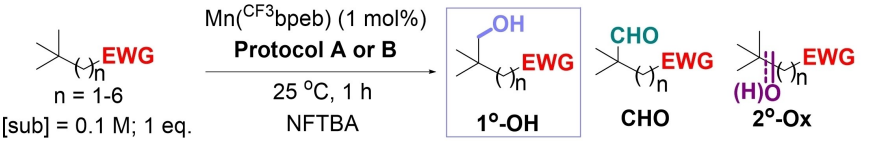
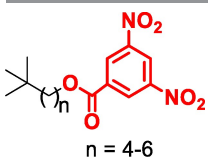
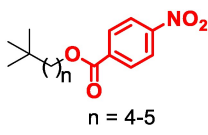

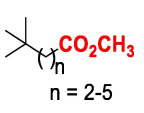
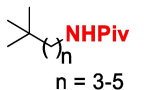
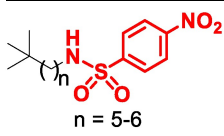
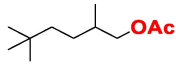
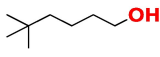
for the C5 and C6 substrates. Notably, the 1° *sr* increased from 1.3 to 2.7 going from C6-OPiv (**14**) to C6-3,5-DNBz (**17**), delivering **P17\_1°-OH** in a synthetically valuable 34 % yield.

With methyl alkanoate esters (*C<sub>n</sub>*-CO<sub>2</sub>CH<sub>3</sub>, **23–26**), results were comparable with those obtained for the corresponding *C<sub>n</sub>*-OPiv substrates, both in terms of 1°-OH yield and 1° *sr*. Primary C–H bond oxidation in C5-CO<sub>2</sub>CH<sub>3</sub> (**26**) proceeded with 1° *sr*=3.5. We note that this selectivity for the primary site exceeds those reported for remote secondary C–H bond oxidation of methylhexanoate catalyzed by [Fe(pdp)]<sup>2+</sup> in CH<sub>3</sub>CN which delivered ketone products derived from oxidation at the most remote methylenic C4 over C3 in a 2.3:1 selectivity.<sup>[7]</sup> Considering that the primary C–H bonds in **26** are seven carbons away from the EWG, the site-selectivity obtained in the oxidation of this substrate is truly exceptional.

On the contrary, the 1° *sr* drops in the oxidation of amide derivatives. The difference is apparent by directly comparing results from the oxidation of *C<sub>n</sub>*-OPiv **11–13** with the corresponding *C<sub>n</sub>*-NHPiv substrates **27–29**. The decrease in 1° *sr* for the latter series could be restored by changing to a more electron withdrawing group such as 4-nitrobenzenesulfonamide (NHNs) for **30** and **31**. Comparable 1° *sr* values were observed for C6-NHNs (**31**) and C6-3,5-DNBz (**17**).

The reach of this selectivity frame is well exemplified in the oxidation of 1-(2,5,5-trimethyl)hexyl acetate (**32**), that contains both primary, secondary and tertiary C–H bonds. Oxidation was selective for the remote primary C–H bonds with a 1° *sr* of 7.3 and **P32\_1°-OH** obtained in 40 % yield as predominant product. On the other hand, the oxidation of 5,5-dimethyl-1-hexanol C4-OH (**33**) bearing a primary alcohol functionality, illustrates the extent and limitation of the deactivating role of NFTBA in functional groups a priori sensitive to oxidation. Hydroxylation of the *tert*-butyl group

**Table 1:** Oxidation of Cn-EWG substrates.

		<div> <b>Protocol A:</b> 4 eq. H<sub>2</sub>O<sub>2</sub> + 17.5 eq. AcOH         </div> <div> <b>Protocol B:</b> 4 eq. urea.H<sub>2</sub>O<sub>2</sub> </div>				
		Protocol	Sub. Conv. (%) <sup>[a]</sup>	Total Yield (%) <sup>[a]</sup>	1°-OH yield (%) <sup>[a]</sup> (Isolated % Yield)	1° sr <sup>[a]</sup>
 n = 4-6	15 (C4)	A	45	37	31 (25)	14.8
	16 (C5)	A	50	40	32 (28)	6.8
	17 (C6)	A	64	52	34 (30)	2.7
 n = 4-5	18 (C4)	A	38	31	26 (22)	11.4
	19 (C5)	A	56	42	32 (26)	5.1
 n = 3-5	20 (C3)	B	31	29	22 (18)	9.8
	21 (C4) <sup>[b]</sup>	A	50	39	33 (31)	13.8
	22 (C5) <sup>[b]</sup>	A	64	48	37 (30)	5.4
 n = 2-5	23 (C2) <sup>[b]</sup>	A	13	11	7 (8)	10.1
	24 (C3) <sup>[b]</sup>	B	54	43	35 (28)	9.7
	25 (C4) <sup>[b]</sup>	A	64	46	38 (32)	9.6
	26 (C5) <sup>[b]</sup>	A	70	54	39 (34)	3.5
 n = 3-5	27 (C3)	A	47	36	27 (24)	4.8
	28 (C4) <sup>[b]</sup>	A	64	42	28 (20)	2.8
	29 (C5) <sup>[b]</sup>	A	79	58	36 (26)	2.2
 n = 5-6	30 (C5)	A	49	35	25 (22)	4.5
	31 (C6)	A	69	42	26 (24)	2.5
 32	32	A	57	50	40 (37)	7.3
 33	33	B	49	38	21 (12)	1.6

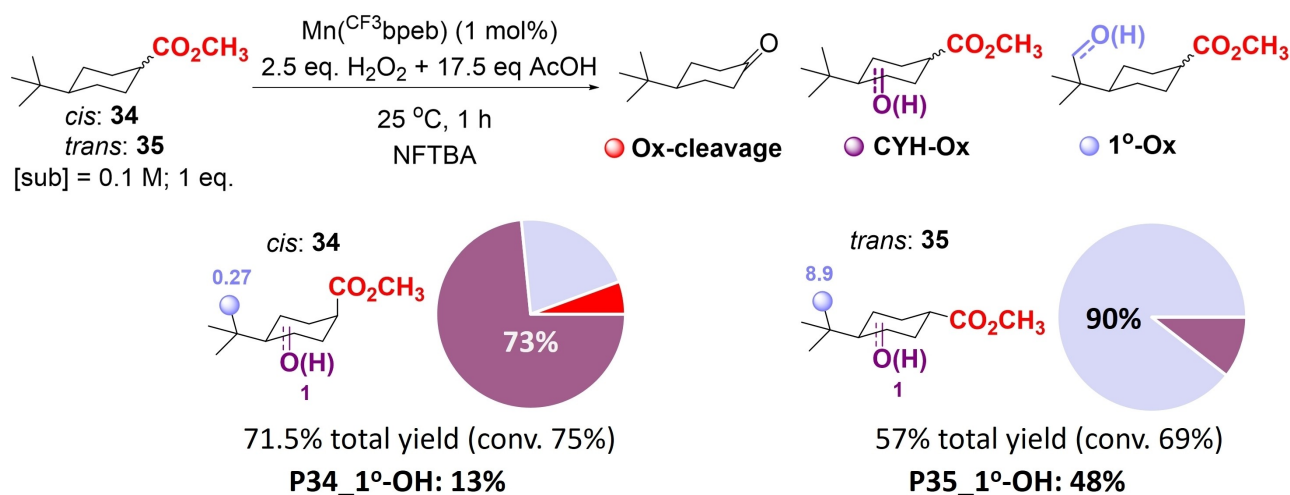
[a] The substrate conversion, product yield and 1° sr were determined by GC-FID with biphenyl as internal standard. Isolated yields are indicated in parentheses. [a] 2 mol % cat. Full reaction details are available in the SI, Tables S31–S67.

is favoured over  $\alpha$ -C–H oxidation, with a 1° sr of 1.6, delivering the diol as the major product (21 % yield).

#### Torsional Effects on the Oxidation of 4-tert-Butylcyclohexane Derivatives

Moving to cyclohexane derivatives, torsional effects were explored as directing tools for *tert*-butyl group oxidation.<sup>[56–57]</sup> Starting with *cis* and *trans* methyl 4-*tert*-butylcyclohexanecarboxylate (*cis*: **34**; *trans*: **35**), oxidation in NFTBA delivered different selectivity profiles (Figure 5). Oxidation of the *cis*-diastereoisomer (**34**), generated a

mixture of cyclohexane oxidation products in overall 56 % yield, including 4 % of *tert*-butylcyclohexanone as C1 oxidative cleavage product (see Figure S2 in the Supporting Information for full details of the product distribution). **P34\_1°-OH**, deriving from *tert*-butyl C–H bond hydroxylation, was formed as a minor product in 13 % yield. Instead, oxidation of the *trans* diastereoisomer occurred with high 1° sr (8.9), delivering **P35\_1°-OH** in 48 % yield. The remarkable site-selective *tert*-butyl C–H bond hydroxylation in **35** can be explained in terms of an effective deactivation of the cyclohexane C–H bonds dictated by electronic, torsional and steric effects, thus enforcing *tert*-butyl as the preferential site for oxidation. Torsional effects account, in addition to



**Figure 5.** Oxidation of *cis* and *trans* methyl 4-*tert*-butylcyclohexanecarboxylates (**34** and **35**). Substrate conversion and product yields were determined by GC-FID with biphenyl as internal standard. The pie charts indicate site-selectivity. Full reaction details are available in the SI, Tables S68–S71.

electronic ones, for deactivation of the  $\text{C}_2\text{--H}$  and axial  $\text{C}_1\text{--H}$  bonds in **35** because HAT from these sites would result in planarization of the incipient carbon radical forcing unfavourable eclipsed conformations.<sup>[56,58]</sup> The same rationale associated to a greater extent of such deactivation imposed by the bulkier *tert*-butyl group holds for the  $\text{C}_3\text{--H}$  and  $\text{C}_4\text{--H}$  bonds. The facile elaboration of the resulting products was shown by converting **P35\_1°-OH** to the chiral  $\gamma$ -lactone, **P35\_Lac** in 96 % yield ( $\text{dr}=5.8$ ;  $ee$  for the major is 65 %) through Jones oxidation followed by Mn-catalyzed carboxylic acid directed  $\gamma$ -lactonization (see Figure S4 in the Supporting Information for full details).

Based on this finding, the oxidation of a series of *trans* 1-EWG-4-*tert*-butylcyclohexanes, **36–46** was explored, aiming at selectively hydroxylating the *tert*-butyl  $\text{C--H}$  bonds (Figure 6). Encouragingly, oxidation of these substrates consistently resulted in remarkable site- and product selectivities, with the corresponding primary alcohol derived from *tert*-butyl  $\text{C--H}$  bond hydroxylation observed as the major product in satisfactory yield. Cyclohexane derivatives **35–39** feature the same number of carbon atoms between the *tert*-butyl and the EWG as their acyclic C4-EWG analogues, and were all hydroxylated at the primary  $\text{C--H}$  bonds with high site-selectivity ( $\geq 90\%$ ). Of notice, for substrates that contain bulky EWGs (**36–39**), significant improvements in  $1^\circ sr$  were observed when compared to the corresponding C4-EWG substrates. For example,  $1^\circ sr$  increases substantially from 2.8 in C4-NHPiv (**28**) to an excellent 19.8 in **37** characterized by the presence of the same group. This drastic enhancement can be explained in terms of the steric shielding and torsional effect exerted by the bulky EWG on the  $\text{C}_2\text{--H}$  bonds. Within these substrates, the highest selectivity for primary  $\text{C--H}$  oxidation was observed for **39** ( $1^\circ sr$  28.1) which bears the bulky and strongly EW 3,5-DNBz. For 4-*tert*-butyl cyclohexanone (**40**), the presence of the carbonyl group in the cyclohexane ring exerts an additional electronic deactivation which translates into a

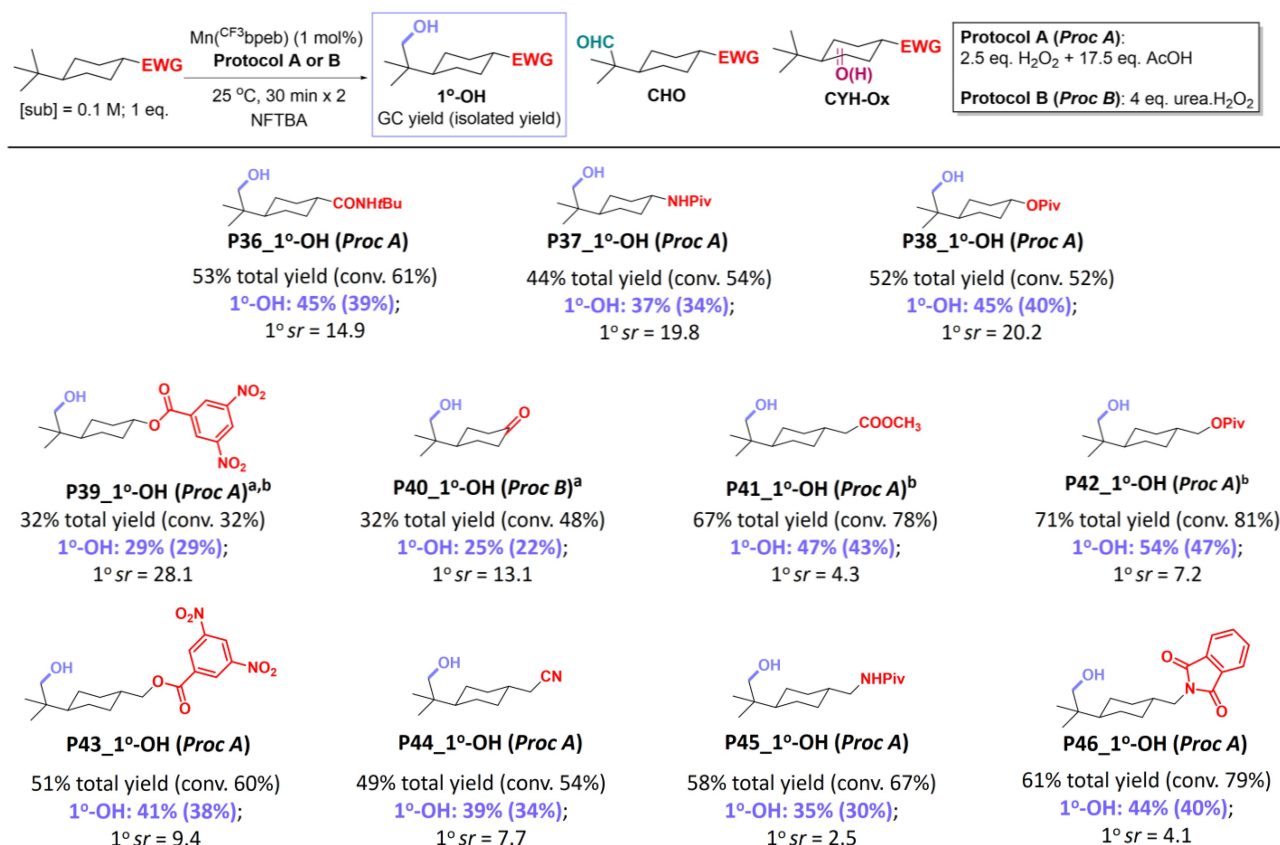
modest yield of **P40\_1°-OH** (25 %). However, a high  $1^\circ sr$  (13.1) was still achieved. Moreover, recycling of NFTBA was accomplished via distillation at the end of the reaction. The recycled solvent was then utilized in the catalytic oxidation of **36** providing analogous results (see SI, section 8 for the details about recycling and reuse of NFTBA).

Interestingly, the high  $1^\circ sr$  observed in the oxidation of these substrates is maintained when the EWGs are moved one methylenic unit away from the cyclohexane scaffold (**41–46**), and remains comparatively higher than the selectivities observed for acyclic C5-EWG substrate analogues. Of notice, because of the improvement in  $1^\circ sr$ , with **42**, bearing the  $\text{CH}_2\text{OPiv}$  group at C1, a notable 54 % yield of the  $1^\circ\text{-OH}$  product **P42\_1°-OH** was obtained. As previously noticed, simple amides exert a weaker deactivation. Thus, oxidation of amide containing derivatives **45** and **46** led to significantly smaller  $1^\circ sr$  values (2.5 and 4.1, respectively). Moreover, the aldehyde product (8 %) resulting from oxidation at the methylenic spacer was observed in the oxidation of **45**.

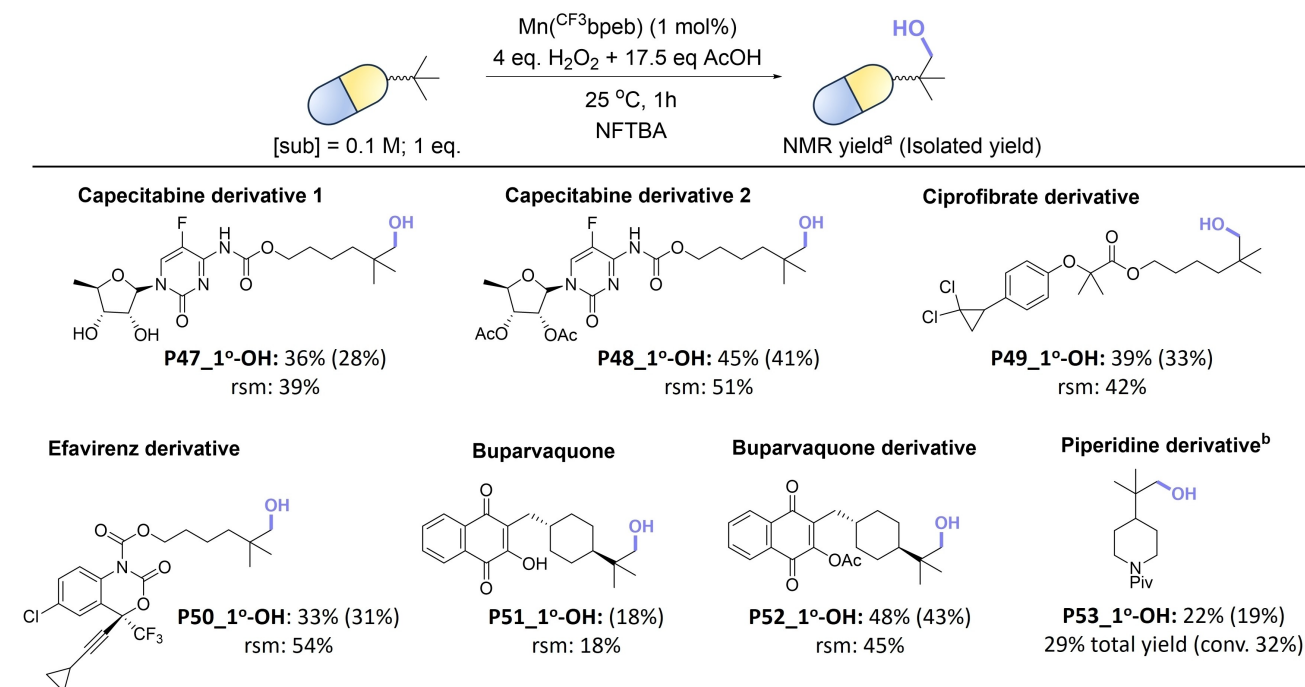
#### Late-Stage Hydroxylation of *tert*-Butyl Containing Pharmaceuticals

With a general understanding of the selectivity factors in hand, a valuable guideline for selective *tert*-butyl hydroxylation in complex molecular settings was established. We notice that this is a common metabolic pathway in drugs possessing *tert*-butyl groups.<sup>[59–61]</sup> Developing a synthetic methodology for *tert*-butyl hydroxylation could offer then a convenient pathway for accessing these drugs. Consequently, the oxidation of complex molecules of pharmaceutical interest containing a *tert*-butyl group (Figure 7) was explored. Capecitabine is an approved anticancer medication that contains a pentyl carbamate. Oxidation of its 1-(5,5-dimethylhexyl) carbamate derivative (**47**) led to a satisfac-





**Figure 6.** Oxidation of 1-EWG-4-*tert*-butylcyclohexanes. Substrate conversion, product yield and 1° sr were determined by GC-FID with biphenyl as internal standard. Isolated yields are indicated in parentheses. [a] 2 mol % cat. [b] 4 eq.  $\text{H}_2\text{O}_2$ . Full reaction details are available in the SI, Tables S72–S93.



**Figure 7.** Late-stage hydroxylation of *tert*-butyl containing pharmaceuticals. [a] 1,3,5-trimethoxybenzene as internal standard. [b] Substrate conversion and product yield were determined by GC-FID with biphenyl as internal standard.

tory 28 % isolated yield of **P47\_1°-OH** and 39 % recovered starting material (rsm). We reasoned that the presence of the 1,2-diol unit on the cyclic ether could potentially inhibit the catalyst through chelation of the metal and was thus protected by acetylation (**48**). With this protection, the corresponding product **P48\_1°-OH** was obtained in a notable 41 % isolated yield accompanied by 51 % rsm, displaying an excellent mass balance. The 1°-OH products were also obtained from oxidation of the 1-(5,5-dimethylhexyl) acetate derivative of Ciprofibrate (**49**) and 1-(5,5-dimethylhexyl) carbamate derivative of Efavirenz (**50**) in 33 % and 31 % isolated yield, respectively. We further examined the oxidation of Buparvaquone (**51**) which is an antiprotozoal drug that contains a *trans* 4-*tert*-butylcyclohexane moiety. Although the hydroxynaphthoquinone unit is highly oxidation and pH sensitive, which in principle is not favourable in our acidic catalytic condition, 18 % of the corresponding hydroxylation product **P51\_1°-OH** could still be isolated. The yield could be greatly improved if the enol functionality was protected by acetylation (**52**), leading to **P52\_1°-OH** in 43 % isolated yield. This system resembles the *trans* 4-*tert*-butylcyclohexane derivatives displayed in Figure 6 where remote *tert*-butyl oxidation was dictated by the combination of torsional and steric effects. In addition, it must be further highlighted that rsm accounted for most of the mass balance of the reactions, further crediting the synthetic utility of these reactions. Lastly, we examined the oxidation of 4-(*tert*-butyl)piperidine derivative (**53**) as such heterocyclic systems are prevalent throughout FDA approved drugs.<sup>[62]</sup> We could obtain **P53\_1°-OH** in 19 % isolated yield which represents a significant improvement when compared to the previously reported platinum-catalyzed C–H oxidation of 4-(*tert*-butyl)piperidine (employed in a 5-fold excess) that yielded < 5 % of the *tert*-butyl C–H oxidation product.<sup>[21]</sup>

## Conclusion

This work pioneers site-selective non-directed hydroxylation of remote primary C–H bonds in *tert*-butyl groups employing hydrogen peroxide and the highly electrophilic Mn(<sup>CF3</sup>bpeb) catalyst in NFTBA. The strong HBD ability of NFTBA enhances the electrophilicity of the Mn-oxo overcoming the high BDE of *tert*-butyl C–H bonds. In addition, both polarity enhancement and polarity reversal effects exerted by this solvent enable highly site-selective and product chemoselective hydroxylation of primary C–H bonds, allowing isolation in synthetically amenable yields of the 1°-OH products that can be diversely elaborated by conventional methods.<sup>[63–66]</sup> The synergistic interplay of steric, electronic, medium and torsional effects operating in the HAT step, enforces selectivity for oxidation of *tert*-butyl C–H bonds over weaker secondary and tertiary ones. Capitalizing on high-valent metal-oxo catalysis, this understanding provides valuable guidelines for expanding the horizon of non-directed C(sp<sup>3</sup>)–H oxidation from secondary and tertiary C–H bonds toward the uncharted domain of primary ones. These guidelines serve as the cornerstone for

late-stage functionalization of *tert*-butyl containing molecules of pharmaceutical interest.

Remarkably, the selective hydroxylation of *tert*-butyl groups emerges as more than an atomic transformation from C–H to C–O, offering an innovative approach for molecular disconnection. It installs the chemically versatile primary alcohol functionality adjacent to a *gem*-dimethyl moiety, uncovering *tert*-butyl as an unprecedentedly recognized functional group more than just a sterically encumbered structural motif.

## Author Contributions

S.-C.C. initiated the project, designed the substrate scope, and performed the experimental works. A.P. developed the catalyst, [Mn(<sup>CF3</sup>bpeb)(OTf)<sub>2</sub>] and assisted for substrate synthesis. M.C. and M.B. directed the experimental part of the project. All authors participated in the writing of the manuscript.

## Acknowledgements

Economic support from European Research Council, (AdvG 883922 to M.C.) Spain Ministry of Science, (MINECO, PID2021-129036NB-I00 to M.C.), (MINECO, PRE2019-090149 to A.P.). Generalitat de Catalunya, (2021 SGR 00475). We acknowledge STR of UdG for experimental support.

## Conflict of Interest

Authors declare that they have no competing interests.

## Data Availability Statement

The data that support the findings of this study are available in the supplementary material of this article.

**Keywords:** C-H hydroxylation • manganese • homogeneous catalysis • hydrogen peroxide • fluorinated alcohol solvents

- [1] M. S. Chen, M. C. White, *Science* **2007**, *318*, 783–787.
- [2] J. Genovino, D. Sames, L. G. Hamann, B. B. Touré, *Angew. Chem. Int. Ed.* **2016**, *55*, 14218–14238.
- [3] M. C. White, J. Zhao, *J. Am. Chem. Soc.* **2018**, *140*, 13988–14009.
- [4] M. Milan, M. Salamone, M. Costas, M. Biatti, *Acc. Chem. Res.* **2018**, *51*, 1984–1995.
- [5] S. Chakrabarty, Y. Wang, J. C. Perkins, A. R. H. Narayan, *Chem. Soc. Rev.* **2020**, *49*, 8137–8155.
- [6] L. Guillemard, N. Kaplaneris, L. Ackermann, M. J. Johansson, *Nat. Chem. Rev.* **2021**, *5*, 522–545.
- [7] M. S. Chen, M. C. White, *Science* **2010**, *327*, 566–571.
- [8] T. Newhouse, P. S. Baran, *Angew. Chem. Int. Ed.* **2011**, *50*, 3362–3374.

- [9] H. M. L. Davies, K. Liao, *Nat. Chem. Rev.* **2019**, *3*, 347–360.
- [10] G. Xia, J. Weng, L. Liu, P. Verma, Z. Li, J.-Q. Yu, *Nat. Chem.* **2019**, *11*, 571–577.
- [11] M. Costas, *Chem. Rec.* **2021**, *20*, 4000–4014.
- [12] A. Ruffoni, R. C. Mykura, M. Bietti, D. Leonori, *Nat. Synth.* **2022**, *1*, 682–695.
- [13] Z. Lu, M. Ju, Y. Wang, J. M. Meinhardt, J. I. M. Alvarado, E. Villemure, J. A. Terrett, S. Lin, *Nature* **2023**, *619*, 514–521.
- [14] M. M. Mayer, *Acc. Chem. Res.* **2011**, *44*, 36–46.
- [15] J. F. Hartwig, M. A. Larsen, *ACS Cent. Sci.* **2016**, *2*, 281–292.
- [16] J. He, M. Wasa, K. S. L. Chan, Q. Shao, J.-Q. Yu, *Chem. Rev.* **2016**, *117*, 8754–8786.
- [17] X.-S. Xue, P. Ji, B. Zhou, J.-P. Cheng, *Chem. Rev.* **2017**, *117*, 8622–8648.
- [18] J. C. K. Chu, T. Rovis, *Angew. Chem. Int. Ed.* **2018**, *57*, 62–101.
- [19] P. Bisel, L. Al-Momani, M. Müller, *Org. Biomol. Chem.* **2008**, *6*, 2655–2665.
- [20] B. R. Cook, T. J. Reinert, K. S. Suslick, *J. Am. Chem. Soc.* **1986**, *108*, 7281–7286.
- [21] M. Lee, M. S. Sanford, *J. Am. Chem. Soc.* **2015**, *137*, 12796–12799.
- [22] F. Juliá-Hernández, T. Moragas, J. Cornella, R. Martin, *Nature* **2017**, *545*, 84–89.
- [23] H. Sommer, F. Juliá-Hernández, R. Martin, *ACS Cent. Sci.* **2018**, *4*, 153–165.
- [24] X. Li, X. Yang, P. Chen, G. Liu, *J. Am. Chem. Soc.* **2022**, *144*, 22877–22883.
- [25] S. Lepri, L. Goracci, A. Valeri, G. Cruciani, *Eur. J. Med. Chem.* **2016**, *121*, 658–670.
- [26] C. R. Zwick III, H. Renata, *ACS Catal.* **2023**, *13*, 4853–4865.
- [27] L. A. Harwood, Z. Xiong, K. E. Christensen, R. Wang, L. L. Wong, J. Robertson, *J. Am. Chem. Soc.* **2023**, *145*, 27767–27773.
- [28] R. V. Ottenbacher, E. P. Talsi, K. P. Bryliakov, *Chem. Rec.* **2018**, *18*, 78–90.
- [29] W. Sun, Q. Sun, *Acc. Chem. Res.* **2019**, *52*, 2370–2381.
- [30] L. Vicens, G. Olivo, M. Costas, *ACS Catal.* **2020**, *10*, 8611–8631.
- [31] J. Chen, Z. Jiang, S. Fukuzumi, W. Nam, B. Wang, *Coord. Chem. Rev.* **2020**, *421*, No. 213443.
- [32] V. Dantignana, M. Milan, O. Cussó, A. Company, M. Bietti, M. Costas, *ACS Cent. Sci.* **2017**, *3*, 1350–1358.
- [33] E. Gaster, S. Kozuch, D. Pappo, *Angew. Chem. Int. Ed.* **2017**, *56*, 5912–5915.
- [34] M. Bietti, *Angew. Chem. Int. Ed.* **2018**, *57*, 16618–16637.
- [35] M. Borrell, S. Gil-Caballero, M. Bietti, M. Costas, *ACS Catal.* **2020**, *10*, 4702–4709.
- [36] A. Call, M. Cianfanelli, P. Besalú-Sala, G. Olivo, A. Palone, L. Vicens, X. Ribas, J. M. Luis, M. Bietti, M. Costas, *J. Am. Chem. Soc.* **2022**, *144*, 19542–19558.
- [37] A. Call, G. Capocasa, A. Palone, L. Vicens, E. Aparicio, N. C. Afailal, N. Siakavaras, E. L. Saló, M. Bietti, M. Costas, *J. Am. Chem. Soc.* **2023**, *145*, 18094–18103.
- [38] Y. Morimoto, Y. Shimaoka, Y. Ishimizu, H. Fujii, S. Itoh, *Angew. Chem. Int. Ed.* **2019**, *58*, 10863–10866.
- [39] V. Dantignana, A. Company, M. Costas, *Chimia* **2020**, *74*, 470–477.
- [40] Y. Morimoto, S. Hanada, R. Kamada, A. Fukatsu, H. Sugimoto, S. Itoh, *Inorg. Chem.* **2021**, *60*, 7641–7649.
- [41] S. A. Cook, A. S. Borovik, *Acc. Chem. Res.* **2015**, *48*, 2407–2414.
- [42] Y. Liu, T.-C. Lau, *J. Am. Chem. Soc.* **2019**, *141*, 3755–3766.
- [43] M. Galeotti, M. Bietti, M. Costas, *J. Am. Chem. Soc.* **2024**, *146*, 8904–8914.
- [44] P. L. Hahn, J. M. Lowe, Y. Xu, K. L. Burns, M. K. Hilinski, *ACS Catal.* **2022**, *12*, 4302–4309.
- [45] S. A. Moteki, A. Usui, T. Zhang, C. R. S. Alvarado, K. Maruoka, *Angew. Chem. Int. Ed.* **2013**, *52*, 8657–8660.
- [46] M. Milan, M. Bietti, M. Costas, *ACS Cent. Sci.* **2017**, *3*, 196–204.
- [47] D. Ravelli, M. Fagnoni, T. Fukuyama, T. Nishikawa, T. Ryu, *ACS Catal.* **2017**, *8*, 701–713.
- [48] C. Shu, A. Noble, V. K. Aggarwal, *Nature* **2020**, *586*, 714–720.
- [49] R. Sang, W. Han, H. Zhang, C. M. Saunders, A. Noble, V. K. Aggarwal, *J. Am. Chem. Soc.* **2023**, *145*, 15207–15217.
- [50] L. Chen, K. G. Malollari, A. Uliana, J. F. Hartwig, *J. Am. Chem. Soc.* **2021**, *143*, 4531–4535.
- [51] M. Galeotti, M. Salamone, M. Bietti, *Chem. Soc. Rev.* **2022**, *51*, 2171–2223.
- [52] We thank a reviewer for this suggestion.
- [53] J. D. Griffin, D. B. Vogt, J. DuBois, M. S. Sigman, *ACS Catal.* **2021**, *11*, 10479–10486.
- [54] J. Chen, W. Song, J. Yao, Z. Wu, Y.-M. Lee, Y. Wang, W. Nam, B. Wang, *J. Am. Chem. Soc.* **2023**, *145*, 5456–5466.
- [55] S. Sisti, M. Galeotti, F. Scarchilli, M. Salamone, M. Costas, M. Bietti, *J. Am. Chem. Soc.* **2023**, *145*, 22086–22096.
- [56] M. Milan, M. Bietti, M. Costas, *Org. Lett.* **2018**, *20*, 2720–2723.
- [57] T. Martin, M. Galeotti, M. Salamone, F. Liu, Y. Yu, M. Duan, K. N. Houk, M. Bietti, *J. Org. Chem.* **2021**, *86*, 9925–9937.
- [58] M. Salamone, V. B. Ortega, M. Bietti, *J. Org. Chem.* **2015**, *80*, 4710–4715.
- [59] A. A. Barnett, *The Lancet* **1996**, *348*, 395.
- [60] J. Shen, M. Serby, A. Reed, A. J. Lee, R. Menon, X. Zhang, K. Marsh, X. Wan, O. Kavetskaia, V. Fischer, *Drug Metab. Dispos.* **2016**, *44*, 1139–1147.
- [61] O. Burk, T. Kronenberger, O. Keminer, S. M. L. Lee, T. S. Schiergens, M. Schwab, B. Windshügel, *Mol. Pharmacol.* **2021**, *99*, 184–196.
- [62] E. T. Vitaku, D. Smith, J. T. Njardarson, *J. Med. Chem.* **2014**, *57*, 10257–10274.
- [63] L. De Luca, G. Giacomelli, A. Porcheddu, *Org. Lett.* **2002**, *4*, 553–555.
- [64] K. Tanaka, W. R. Ewing, J.-Q. Yu, *J. Am. Chem. Soc.* **2019**, *141*, 15494–15497.
- [65] X. Liu, X. Rong, S. Liu, Y. Lan, Q. Liu, *J. Am. Chem. Soc.* **2021**, *143*, 20633–20639.
- [66] M. Fang, G. S. Kumar, S. Racioppi, H. Zhang, J. D. Rabb, E. Zurek, Q. Lin, *J. Am. Chem. Soc.* **2023**, *145*, 9959–9964.

Manuscript received: February 8, 2024

Accepted manuscript online: April 30, 2024

Version of record online: June 10, 2024